IgMin Research STEM ISSN: 2995-8067 A Multidisciplinary Open Access Journal

SCIENCE SUBJECT
Biochemistry | TOPIC(S)

Article Information

Submitted: January 01, 2024
Approved: July 17, 2024
Published: July 18, 2024

How to cite this article: Golovanova O. Biomimetic Synthesis of Calcium Carbonate in Bile in the presence of Amino Acids. IgMin Res. July 18, 2024; 2(7): 632-641. IgMin ID: igmin227; DOI: 10.61927/igmin227; Available at: igmin.link/p227

Keywords: Crystallization; Calcium carbonate; Vaterite; Aragonite; Calcite; Human bile; Gallstones; Crystallization; Synthesis; Dissolution kinetics

Research Article

Biomimetic Synthesis of Calcium Carbonate in Bile in the presence of Amino Acids

Olga Golovanova*

Department of Inorganic Chemistry, The Department of Chemistry, Omsk State University is Named after F.M. Dostoevsky, Mira St., 55a. Omsk, 644077, Russia

***Correspondence:** Olga Golovanova, Department of Inorganic Chemistry, The Department of Chemistry, Omsk State University is Named after F.M. Dostoevsky, Mira St., 55a. Omsk, 644077, Russia, Email: golovanoa2000@mail.ru

Abstract

Thermodynamic and experimental modeling of calcium carbonate crystallization in a model solution of human bile has been carried out. The process of calcium carbonate (calcite and vaterite) crystallization from solutions containing bile has been studied. It is shown that differences in the phase and group composition of the samples arise depending on the synthesis parameters. It has been established that in the presence of 1 wt. % bile, calcite is formed, and an increase in the concentration of bile in the initial solution from 5 to 100 wt. % contributes to the crystallization of vaterite. It is shown that the mass of the solid phase increases with an increase in the concentration of bile in the initial solution. The dissolution of the synthesized samples was performed in 0.9 wt. % NaCl solution and 0.05 M EDTA solution. It was found that the presence of bile components in the composition of solid samples reduces the rate of their dissolutions.

Introduction

The influence of a wide range of natural and anthropogenic factors on a living organism results in the formation of pathogenic organo-mineral aggregates that occur in most human organs. Increasing risk factors draw the attention of science to the problem of the etiology of diseases related to pathological biominerals. Primarily physicians, as well as chemists, mineralogists, physicists, and other specialists, are interested in the studies of the reasons for the diseases.

Among the diseases of the human digestive system, a special place is occupied by cholelithiasis (GSD, cholelithiasis), due to its high prevalence. Gallstone disease is a worldwide problem, the solution of which lies in a detailed study of the physicochemical mechanisms of lithogenic bile and gallstone formation. Despite a gradual decrease in mortality due to gallbladder disease, there is a steady increase in the incidence of cholelithiasis. It is known that over the past five years, more than 10% of the world's population has been suffering from cholelithiasis. If such an increase in the incidence rate continues, this figure will increase to 20% by 2050 [1-4]. In terms of prevalence among all diseases of a modern human, cholelithiasis occupies a leading position, second only to cardiovascular pathology and diabetes mellitus. However, among diseases of the digestive system, cholelithiasis ranks first, according to several scientists.

Currently, the physicochemical causes and mechanisms of gallstone formation have not been fully determined, however, there are several theories accepted by the scientific community based on data on the composition of gallstones. According to the provisions of the micellar theory of bile cholesterol transport and its physical and chemical substantiations, the process of formation of cholesterol stones includes the following stages: supersaturation of bile with cholesterol, nucleation and precipitation of cholesterol monohydrate crystals (through the stage of formation and agglomeration of liquid crystals), aggregation of crystals into microlites and their growth at further crystallization [5,6]. In this case, the dispersed characteristics of the precipitates formed depend on the degree of supersaturation and crystallization conditions [7-9].

However, according to some scientists, the level of supersaturation of bile with cholesterol, which is achieved in reality, is not enough for the formation of "pure" cholesterol crystallization nuclei: spontaneous nucleation of cholesterol requires very supersaturated solutions with a supersaturation of about 300%. Such a concentration of cholesterol in bile is physiologically impossible for a person. Therefore, the formation of nuclei of cholesterol crystalline stones occurs as a result of heterogeneous crystallization with the participation of calcium salts, bilirubin, etc. [9-12].

ISSN 2995-8067 DOI: 10.61927/igmin227

A correlation between cholelithiasis incidence and changes in concentrations of some organic components of bile has been proven. For instance, the evaluation of protein content in real bile samples was performed by determining the amount of total nitrogen [13,14]. It turned out that the nitrogen concentration range in cholelithiasis bile was 1.50 to 1.80 wt.%, which is about 3 times higher than the nitrogen content in the bile of a healthy person (0.48 wt.%). The increase in the share of total nitrogen is probably related to the concentration growth of not only amino acids but also nitrogen-containing organic compounds like bilirubin and phospholipids.

The contents of most inorganic components in pathogenic bile are also increased, namely, the mass fraction of sodium is 1.2 times higher than its content normal, phosphorus and potassium - 1.5 times, calcium - 2.5 times, magnesium - 4.5 times; iron content is 3.5 times less than the norm. It is known that calcium cations play a cementing role in the cholesterol nucleation process and are precipitated from bile in the form of carbonates, palmitates, and phosphates. Thus, deviations in elemental and molecular compositions of pathogenic bile, apparently lead to disruption of its colloidal structure that promotes coagulation of cholesterol and the formation of stones.

The processes of calcium carbonate precipitation in biological fluids (particularly in bile) are complicated, so a solution to the problem of stone genesis in bile-containing media is not only of medical significance. It also holds scientific interest from the viewpoint of determination of the physicochemical properties of these compounds [15-20].

The reasons for the selective crystallization of $CaCO_3$ polymorphous modification in pathogenic mineralization are of a complicated nature determined by the specificity of physicochemical and kinetic factors governing the formation of stones. In turn, the formation of calcium carbonate crystals as nucleation centers in bile saturated with cholesterol may promote cholesterol crystallization and the formation of gallstones. Thus, experimental modeling of these conditions is an urgent and significant task.

Among all the polymorph modifications of $CaCO_3$, vaterite is formed to a great extent in gallstones due to the crystallization conditions [5,21,22]. Moreover, vaterite is thermodynamically unstable and seeks to be transformed in stable calcite modification. This feature of the phase composition of gallstone inorganic components is of significant interest since research in this field can elucidate the true causes of gallstone formation and help in the development of new drugs and ways to prevent this disease.

To study the physicochemical conditions of crystallization and the phase composition of calcium carbonate polymorphs formed in the real settings of the human body, it is possible to use thermodynamic modeling methods [23-25], as well as synthesis and characterization of $CaCO_3$ samples [26,27]. To approximate the model of the bile system to the real parameters and to simulate its various states in this study, we use precursor concentrations, which are the norm for a healthy average person [5,28]. The variations of these concentrations may correspond to various pathological changes in the state of human bile.

This work is aimed at the thermodynamic and experimental modeling of calcium carbonate crystallization from a bile solution by varying the solution composition (precipitating ions, amino acids, albumen) and experimental parameters (concentrations of substances introduced into the system).

Experimental section

Thermodynamic modeling: Was carried out using a theoretical model of the formation of a solid phase in the Ca^{2+}–CO_3^{2-} system in human bile. We considered a hypothetical solution where the content of inorganic components, pH, ionic strength, and temperature corresponded to the average respective values for the bile of an average adult and healthy person (Table 1) [5,29,30]. The effect of organic components of bile on crystallization was not taken into account.

The theoretical characteristics of calcium carbonate formation as a solid phase in solution are the reference values of the solubility product at 298 K, recalculated to 310 K according to the Van-Goff isobar equation: $K^0_{sp,310}$(vaterite) = $1.01 \cdot 10^{-8}$ and $K^0_{sp,310}$(calcite) = $2.7 \cdot 10^{-9}$ [25,31].

$$K_{sp}^{0\,cond} = \frac{K_{sp}^{0}}{\gamma_A^x \cdot \gamma_B^y \cdot x_A^x x_B^y} \quad (1)$$

The conditional solubility products were calculated taking into account the activity coefficients of ions and the occurrence of protolysis and complexation of precipitate-forming ions.

At SI > 0 and ΔG < 0, the solution is supersaturated concerning its thermodynamic equilibrium state, as a result of which a crystalline phase is formed. All of the physicochemical processes occurring in the studied system were taken to be steady-state and isothermal (T = 310 K). All necessary calculations were carried out in Microsoft Excel 2013 software, and the diagram was plotted in OriginPro 2018.

Table 1: Ion contents in bile [6].

Parameter	Value		
	min	avg.	max
pH	6.5	7.25	8.0
C, mmol/L			
Na^+	130	205	280
K^+	2.7	8.85	15.0
Ca^{2+}	1.2	6.6	12.0
Mg^{2+}	1.3	2.15	3.0
Cl^-	14.5	70.25	126
HCO_3^-	8.0	31.5	55

$$\Omega = \left(\frac{IAP}{K_S^O} \right)^{\frac{1}{p+q}} \quad (2)$$

$$SI = lg(\Omega) \quad (3)$$

Here, K_s/ - conditional product of solubility of the compound (characterizes the equilibrium position taking into account the total influence of electrostatic and chemical interactions); IAP - product of ion concentrations in solution to the extent of their stoichiometric coefficients involved in the formation of this poorly soluble compound.

In this case, if the calculated value of the supersaturation index SI for a compound is greater than zero, then under these conditions, the precipitation of this phase from the solution is thermodynamically likely.

The possibility of precipitation of a sparingly soluble compound from solution was also evaluated by the value of the Gibbs energy of crystallization:

$$\Delta G = -\frac{RT}{\nu} \cdot \ln \frac{IAP}{K_S^0} \quad (4)$$

Here, R is the universal gas constant, J/mol-K, and T is the absolute temperature, K.

The synthesis of calcium carbonate: Was carried out through precipitation from the aqueous solution (experiment 1) and the bile solution with variations of its concentration (experiment 2) by the reaction:

$$CaCl_2 + 2NaHCO_3 \rightarrow CaCO_3\downarrow + 2NaCl + CO_2 + H_2O \quad (5)$$

The precipitate was obtained by mixing the solution of calcium chloride ($CaCl_2 \cdot 2H_2O$, pure for analysis reagent grade) and sodium hydrocarbonate ($NaHCO_3$, chemically pure reagent grade) in equimolar concentrations at room temperature (25 °C). Initial reagents were the salts, twice distilled water, and bile (preserved medical bile, PC Samson-Med, Russia). Bile concentration was varied from 1 to 100 mass % with a step of 5 %. In each experiment, acidity (pH) was corrected to 7.0±0.1 by adding a solution of hydrochloric acid (1 mol/L).

All samples were kept during the synthesis in a Biotron-4 thermostat box (SibFTI, Russia) at a temperature of 37 °C, which corresponds to the average temperature of human organs. After settling the heterogeneous system for 24 h to 12 days, the solution was filtered with a step of 24 h, the precipitate on the filter was washed with water (volume V = 50 mL), and dried in the drying box at a temperature of ~80 °C to the constant mass. Then the precipitate was weighted and transferred into the marked container.

Synthesis of calcium carbonate in the presence of organic compounds: Preserved medical bile, a 250-mL sample, was divided into two equal portions (125 mL each). Then certain quantities and additive concentrations are added to the first portion, the concentrations of which are given in Table 2, and Ca2+ was added to the second portion (Table 2).

After the added substances dissolved, the first solution with the additive was poured from a burette at a rate of ~0.15 mL/s to the second solution, which was thermostated in a beaker at 310 ± 1 K, under continuous stirring. After the mixing was complete, the thus-obtained solution (250 mL) was stirred for another 30 min.

Many researchers emphasize that the specificity of the organic component controls to a great extent the phase formation in human organisms [32-34]. In this context, an urgent problem is to investigate the organic component of pathogenic OMAs.

Syntheses in the presence of glycine and glutamic acid: The amounts of Ca^{2+} ions, glycine, and glutamic acid to be added were calculated from average Ca^{2+} concentrations in bile (Table 1) and average amino acid concentrations in human blood serum referred to 250 mL of the final solution [35-37].

$CaCO_3$ syntheses in the presence of albumen: The weight of albumen added was varied based on the average protein content in bile (from 0.025% to 0.14%, i.e., 0.083% by weight on the average) and in the doubled average concentration [23].

$CaCO_3$ synthesis in the presence of albumen and the twenty essential amino acids (EAAs): The amounts of $CaCl_2 \cdot 2H_2O$, $NaHCO_3$, and EAAs to be added were calculated concerning the maximal values from Tables 1,2, respectively, referred to the 250 mL of the final solution.

The resulting solutions were placed in a Biotron-4 thermostat box maintained at 310±1 K for 120 h. The thus-obtained precipitates were filtered, washed, and dried at room temperature until a constant weight was acquired and until chemically unbound water was completely removed.

X-ray powder diffraction: Characterization of prepared samples was performed using a D8 Advance (Bruker) diffractometer. X-ray diffraction patterns were recorded in

Table 2: Contents of major components and additives used in synthesis.

Sample no.	Component, mol		Additive
	$CaCl_2 \times 2H_2O$	$NaHCO_3$	
1	1.65×10^{-3}	7.88×10^{-3}	Glycine, 6.25×10^{-5} mol
2			Glutamic acid, 2.86×10^{-5} mol
3			Albumen, 0.21 r
4			Albumen, 0.42 r
5	3.00×10^{-3}	13.8×10^{-3}	20 EAAs (according to Table 1) and albumen, 0.35 g

ISSN 2995-8067 DOI: 10.61927/igmin227

the range of 5°–80° 2θ angles. The qualitative phase analysis of samples was carried out concerning PDF-2.

IR spectra of solid phases were recorded on an FT-801 (Symex) spectrometer. A 0.5-mg powdery sample was mixed with 50 mg KBr and compacted into a disk-shaped tablet of 3 mm diameter at room temperature. The spectral resolution was 4 cm^{-1}; the total number of scans was 32. The spectra of tested samples were recorded in the range from 400 to 4000 cm^{-1}. The IR spectra were processed in the software OriginPro 2018 and concerning the literature data on the absorption peak positions for atomic groups [38].

The specific surface area of two solid samples (one sample from each experiment 1 and 2) was studied using single-point nitrogen adsorption at 77.4 K with the help of a Sorbtometr adsorption analyzer (LC Katakon). The values of specific surface (m_2/g) were calculated according to Brunauer–Emmett–Teller (BET) procedure with a 5 % error.

Dissolution characteristics of the synthesized samples were investigated in two solvents to simulate the extracellular fluid of a human organism: sodium chloride (NaCl, 0.9 mass %) – as a model solution, and ethylenediamine tetraacetic acid (EDTA, 0.05 mol/L) – as an efficient solvent for calcium compounds. The dissolution kinetics for the samples of the obtained solid phases, 0.1000±0.0001 g in mass (the samples were weighted with analytical balance with the accuracy of 0.1 mg) was studied in a thermostated cell at 37 C for 2 h with the constant volume of the liquid phase under permanent mixing. The parameters that were controlled during the experiment included acidity (pH), the concentration of calcium ions that passed into the liquid phase (pCa), and dissolution time (t) for calcium carbonate. The concentration of calcium ions was determined through direct potentiometry with the help of an I-160MI ionometer using a Ca-selective electrode. Kinetic curves were plotted based on obtained experimental data, and mathematical processing of the data was carried out according to the algorithm described in [39].

Results and discussion

The thermodynamic modeling

Of solid phase formation in the Ca^{2+}– system initially ignored Ca^{2+} complexation but accounted only for the protolytic interactions of calcite and vaterite. Based on the calculated data in the pH range from 5.0 to 9.0 units (the physiological norm of bile pH is the range from 6.5 to 8.0 units [23,328,40]) and when varying the concentrations pC of Ca^{2+} ions and CO_3^{2-} 0.5 to 6.0 units diagrams of functional dependences SI = f(pCa^{2+}; pCO_3^{2-}) were plotted at different pH values of the model solution. For clarity, Figure 1 shows two such diagrams: at pH = 5 and pH = 9. For the corresponding values of the supersaturation indices, the values of ΔG were calculated with varying pH, and the diagrams of the dependences ΔG = f(pCa^{2+}; pCO_3^{2-}) were plotted, in Figure 2 shows diagrams at pH = 5 and pH = 9.

The calcium carbonate stability field was rapidly designed as pCa^{2+} = *f*(pH). These were three-dimensional diagrams (surfaces) that described precipitation equilibrium at *SI* = 0, above which any figurative point of the system under study described its state as an ideal solution (no solid phase is formed; *SI* < 0), and below this surface, it describes the state where *SI* > 0 (a precipitate is formed). The diagram obtained for calcite appears in Figure 3.

No qualitative distinctions were found between the calcite and vaterite stability fields; however, all pCa^{2+} values obtained for vaterite are at a shift of about 0.35 to the negative side. This

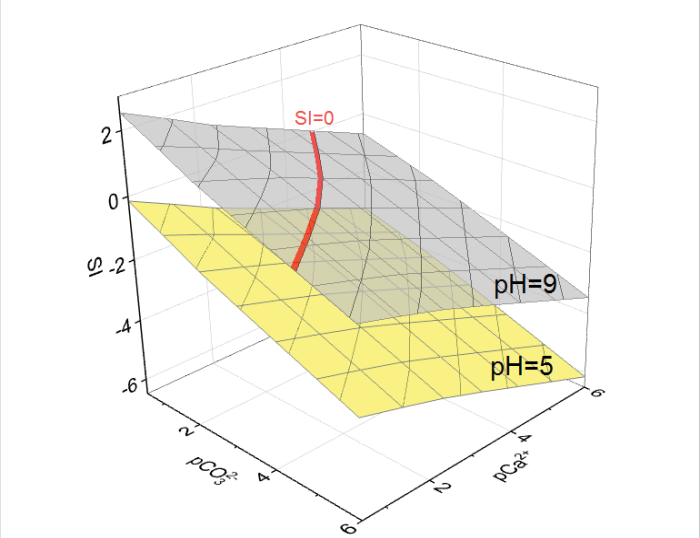

Figure 1: Diagrams of dependence of SI on pCa2+ and pCO32– in a model solution at pH = 5 and 9.

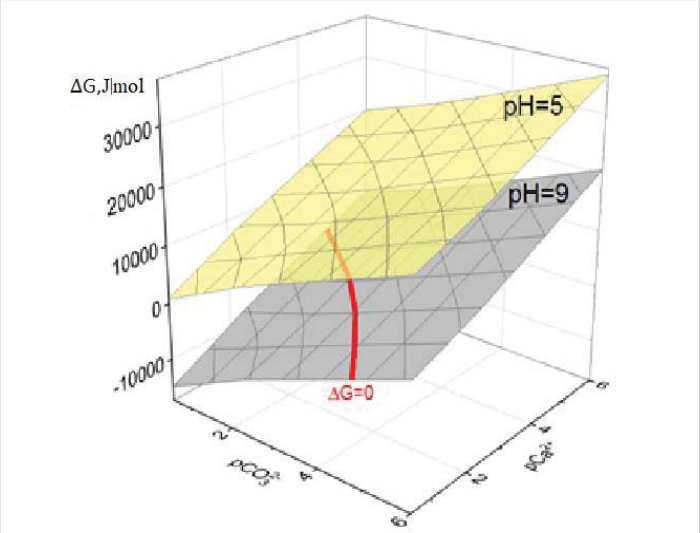

Figure 2: Diagrams of dependence of ΔG on pCa2+ and pCO32– in a model solution at pH = 5 and 9.

ISSN 2995-8067 DOI: 10.61927/igmin227

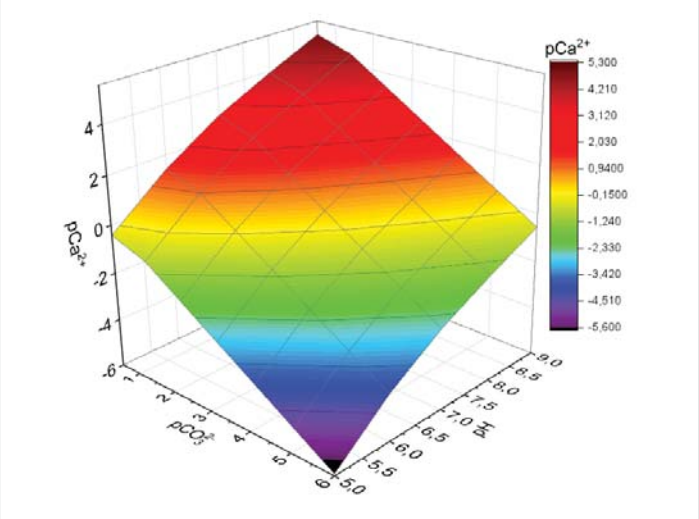

Figure 3: Calcite stability field where Ca2+ complexation is ignored.

indicates that vaterite formation in a model solution requires higher concentrations of precipitate-forming ions than for calcite if the other conditions are equal. At pH 7.25 and pCa^{2+} = 1.50 (the mineral composition of human bile, Table 1), to the critical point (a point inside the stability field) for calcite, there corresponds $pCa^{2+} \approx 2.13$; for vaterite, $pCa^{2+} \approx 1.78$ [23].

Since calcium carbonate crystallization in bile can be affected by bile amino acids, we carried out analogous calculations taking into account Ca^{2+} complexation with glycine and glutamic acid (separately) using their average serum concentrations and with twenty essential amino acids referred to their maximal permissible serum concentrations (Table 2).

The complexation function was calculated using the stability constants of Ca^{2+} with amino acids [41]. No qualitative changes were noticed upon the formation of a low-solubility compound ($CaCO_3$); thus, the stability field of glycine and glutamic acid in the concentrations created in the model solution remains unchanged. The decrease in pCa^{2+} corresponding to the critical point is less than 0.0005 units.

In the same way, in the case where the model solution is added with all EAAs in their highest concentration, no qualitative changes are observed. Even for pH = 7.25 and pCa^{2+} = 1.50, to the critical point in the diagram, there corresponds $pCa^{2+} \approx 2.13$, a value as little as 0.003 pCa^{2+} units lower than the respective value in the absence of complexation; so, the appearance of the $CaCO_3$ stability field is almost identical to Figure 3.

Because in real bile calcium carbonate crystallization can be affected by bile amino acids, we carried out analogous calculations taking into account Ca^{2+} complexation with glycine and glutamic acid (separately) using their average serum concentrations and with twenty essential amino acids referred to their maximal permissible serum concentrations. The complexation function was calculated using the stability constants of Ca^{2+} with amino acids [41]. No qualitative changes were noticed upon the formation of a low-solubility compound ($CaCO_3$); accordingly, the stability field of glycine and glutamic acid in the concentrations created in the model solution remains unchanged. The decrease in pCa^{2+} corresponding to the critical point is less than 0.0005 units.

The figurative point with the coordinates pH = 7.25; pCa^{2+} = 2.18; and pCO_3^{2-} = 1.50 describes the state of the human bile model solution with average respective values. This point lies above the stability field. The point is characterized by $SI \approx -0.4$. The system in this state is a true solution, which is, however, very close to precipitate formation (especially in the case of calcite). So, equilibrium in the considered system could be easily shifted toward solid phase formation even when excessive Ca^{2+} and HCO_3^- ions would be added in concentrations equal to average physiological concentrations (Table 1), just as it was done during the subsequent synthesis of calcium carbonate.

Synthesis of calcium carbonate

According to the XRD data, independently of the duration of synthesis, the samples synthesized from the aqueous solutions (experiment 1) are represented by the calcite phase. A typical X-ray diffraction pattern of the precipitate contains reflections in angle regions of 23.0, 29.4, 39.5, and 43.0° over 2θ (Figure 4), which corresponds to the line diffraction patterns of calcite [2,42]. It is necessary to stress that calcite precipitated from aqueous solutions contains vaterite as an admixture. This is confirmed by the peak at 26.0° over 2θ. Vaterite content is not more than 5 % (Figure 5).

IR-spectroscopy

The IR spectrum of the synthesized sample (experiment 1,

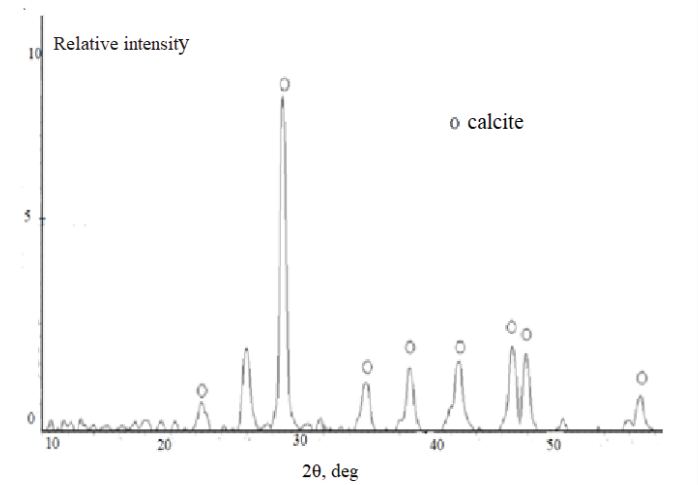

Figure 4: Diffraction patterns of calcium carbonate synthesized from the aqueous medium.

ISSN 2995-8067 DOI: 10.61927/igmin227

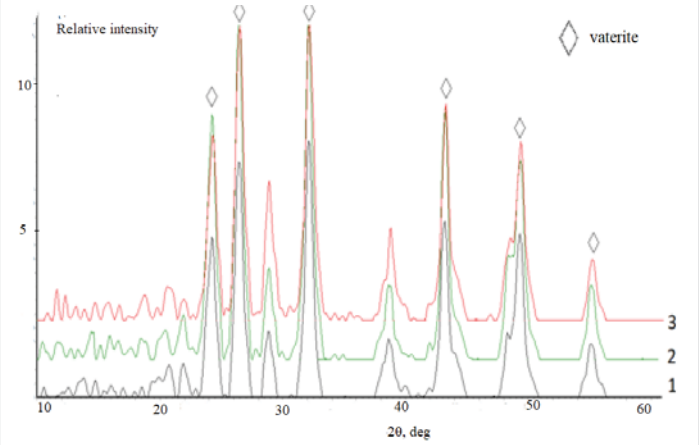

Figure 5: Diffraction patterns of calcium carbonate synthesized the solutions containing, mass %: 1 –10; 2 – 20; 3 – 30. Synthesis time 24 h.

synthesis time 24 h) (Figure 6) contains absorption bands (a.b.) characteristic of carbonate groups which are assigned to bending vibrations in CO_3^{2-} (702 cm^{-1}) and O–C–O bonds in CO_3^{2-} (880 cm^{-1}), stretching antisymmetrical vibrations of C–O bonds in CO_3^{2-} (1407 cm^{-1}). The absorption band at 1795 cm^{-1} corresponds to the high-intensity stretching vibrations of C=O in COOH groups, while the band at 2499 cm^{-1} is due to the low-intensity stretching vibrations of C=O in COOH groups (see Figure 6).

Chemical composition

It was established utilizing low-temperature nitrogen adsorption that the precipitate obtained in the presence of bile (30 mass %) possesses the most developed specific surface area (5 m^2/g) in comparison with calcium carbonate formed from the solution containing no bile (1 m^2/g). An increase in the specific surface area by a factor of 5 occurs due to the inclusion of bile components into the composition of the synthesized samples and by the resulting change in the phase composition of $CaCO_3$. An increase in the mass of precipitate from 0.2 to 0.9 g with an increase in bile concentration in the initial model solution was detected [42].

It is known that the major bile components are biliary acids and bilirubin, which can interact with calcium ions forming the corresponding salts [5,37].

Dissolution kinetics investigation showed that the interaction of the solvent (medium) with the samples involves the release of Ca^{2+} ions and their accumulation in the liquid phase. The concentration of Ca^{2+} increases rapidly in sodium chloride solution (Figure 7) at the initial stage of dissolution. Later on, the intensity of Ca^{2+} ion release into the liquid phase from all samples decreases gradually. In the case of EDTA solution, the concentration of free calcium ions in solution is lower because the formation of EDTA complexes with calcium ions takes place (lgK_{st} = 10.7, where K_{st} is a stability constant of the complex).

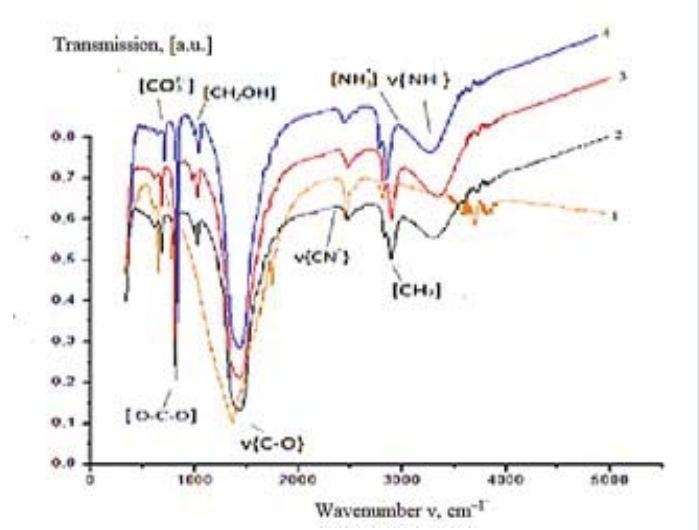

Figure 6: IR spectra of precipitates obtained from solutions with different bile content: 1 – 0, 2 – 10, 3 – 20, 4 – 30 mass %.

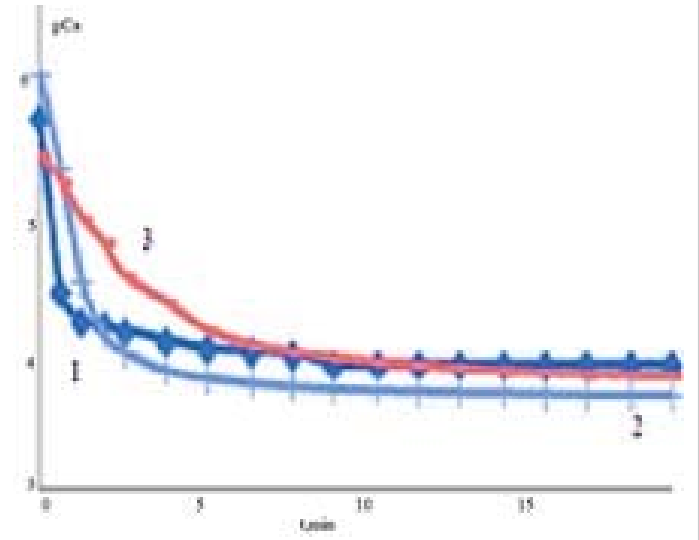

Figure 7: Dependences of calcium concentration (pCa) on the time of dissolution (t) of solid phases (a – 0.9 mass % NaClfor different concentrations of bile in solution: 0 (1), 50 (2), 100 (3) mass %.

The initial values of the rates of calcium release in the solution were calculated based on the obtained experimental dependencies pCa =$f(t)$. The experimental kinetic curve (a change in the concentration of calcium ions) looks like an exponential dependence, dissolution obeys the first-order kinetic equation. Because of this, the rate may be determined as a tangent of the slope of a linear region of the line. One can see (Table 3) that the initial rate of sample dissolution is higher for the samples synthesized from the solutions containing no bile than for the samples synthesized in the presence of bile. It may be assumed that a decrease in the rate of dissolution of calcium carbonate formed in the presence of bile is promoted by the inclusion of the organic components of bile into the solid phase.

ISSN 2995-8067 DOI: 10.61927/igmin227

Table 3: Initial rates (V) of the dissolution of solid phases formed with different bile concentrations in solution.

Bile concentration, mass %		NaCl solution (0.9 mass %)		EDTA solution (0.05 mol/L)	
	Dissolution stages	t, min	$V \cdot 10^5$,min−1	t, min	$V \cdot 10^5$,min−1
0	1	0-1	4.0	0-2	5.0
	2	2-7	4.79	3-6	12.4
50	1	0-2	3.0	0-2	0.02
	2	3-15	7.94	3-6	0.39
100	1	0-4	1.0	0-2	0.01
	2	5-15	5.94	3-7	0.27

Synthesis of calcium carbonate in the presence of organic compounds

The X-ray powder diffraction patterns of the prepared samples showed that the phase compositions of samples 1–4 almost do not differ from one another, while sample 5 has some distinctions. For clarity, Figure 8 shows the diffraction patterns of samples 3 and 5. One can see that sample 3, prepared in the presence of albumen (0.083 wt %), features a broadband (extending from 15° to 55°) corresponding to amorphous $CaCO_3$ (the major phase) and peaks characteristic of minor calcite (23.0°, 29.4°), aragonite (26.3°), and monohydrocalcite (32.0°). In the X-ray diffraction pattern of sample 5, the major phase is vaterite (21.0°, 24.9°, 27.0°, 32.7°, 44.5°, 49.0°, 50.0°, and 56.0°); peaks characteristic of minor calcite (29.4°, and 39.5°) are poorly defined. The peaks located at 21.7° and 20.3° and those to the left of them correspond to organic calcium salts and calcium compounds adsorbed on the $CaCO_3$ surface.

The FT-IR spectroscopic characterization of the prepared calcium carbonate samples correlates with XRD data. Powders 1–4 have nearly identical spectral patterns (Figure 9).

The IR spectra of these samples feature bands due to the C–C stretching vibrations at 1540–1580 cm^{-1} and narrow bands at 2850–2920 cm^{-1}, which correspond to the C–H stretching vibrations. These vibrations are characteristic of the presence of organic molecules in the powder in the form of calcium salts of organic acids and pigments that enter the bile or are adsorbed on the surface of crystallizing particles. The N–H stretching vibrations appearing as a broad band in the region of 3400 cm^{-1} corresponds to the amino group vibrations in bilirubin, amino acids, or proteins adsorbed on the surface of calcium carbonate. The band at 1050–1100 cm^{-1} describes the O–H and C–N stretching vibrations, respectively, in bile pigments and bile cholesterol. The asymmetric stretching vibrations of C–O in CO_2 appear as a peak at 2350 cm^{-1}. The spectra also feature stretching vibrations (at 1650 cm^{-1}) and bending vibrations (at 3740 cm^{-1}) in a water molecule. The spectra of four samples feature vibration bands of identical positions and intensities that correspond to a group of atoms in CO_3^{2-}. These are nondegenerate symmetrical changes in bond lengths ($\nu_1(CO_3^{2-})$) at 1068 cm^{-1}, doubly degenerate deformation of opposite bond angles ($\nu_2(CO_3^{2-})$) at 866–875 cm^{-1}, triply degenerate asymmetrical changes in bond

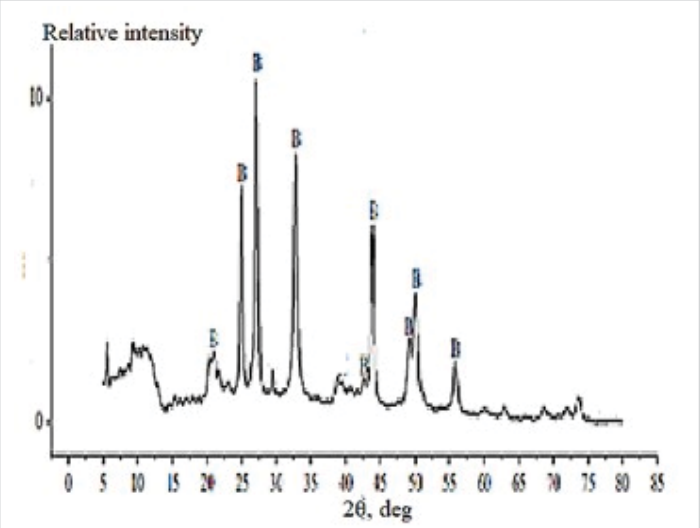

Figure 8: X-ray diffraction patterns of sample 5. B – vaterite.

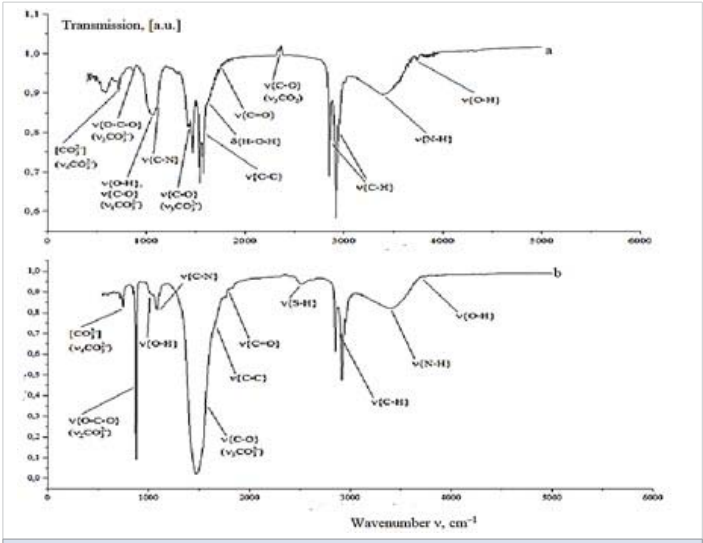

Figure 9: IR spectra of (a) sample 3 and (b) sample 5.

lengths ($\nu_3(CO_3^{2-})$) at 1420–1475 cm^{-1} and triply degenerate asymmetrical changes in one bond length in response to a change in bond angles ($\nu_4(CO_3^{2-})$) at 720 cm^{-1} [38]. This set of characteristic IR frequencies points to the presence of calcite and amorphous $CaCO_3$ in the samples. Thus, no changes have been found in the group structure composition among samples 1–4. A comparison of samples 3 and 4, which were prepared in the presence of various albumen concentrations, showed that a twofold increase in albumen concentration only insignificantly adds to the absorption intensity at 3400 cm^{-1} (N–H vibrations), indicating an enhancement of diverse interactions between albumen and calcium carbonate.

The spectrum of sample 5 has some distinctions from the samples considered above. At 2500 cm^{-1} a band appears corresponding to the S–H stretching vibrations in sulfur-containing amino acid molecules (cysteine, methionine), probably also adsorbed on the surface of the powder. The

vibrations $\nu_3(CO_3^{2-})$ give a high-intensity band at 1440–1490 cm^{-1}, as distinct from those in the previous samples. At 875 cm^{-1}, a well-defined $\nu_2(CO_3^{2-})$ vibration peak appears. The $\nu_4(CO_3^{2-})$ vibrations shift toward 745 cm^{-1}. The set of characteristic frequencies obtained indicates that sample 5 is represented by a vaterite phase [22].

Thus, the results obtained by XRD, FT-IK spectroscopy, and optical microscopy demonstrate that the nature and concentrations of additives in bile, as well as the value of supersaturation of precipitate-forming ions, can affect the nature of crystallizing calcium carbonate phases. Qualitative changes in phase composition are observed in the presence of all EAAs and albumen in combination at their physiologically permissible highest concentration in human bile. Some researchers [43] observe that the presence of aspartic acid and cholesterol during calcium carbonate precipitation from aqueous solutions promotes vaterite formation along with calcite; when exposed to the solution for 96 h, however, the newly formed metastable vaterite almost completely converts to calcite, while in sample 5, vaterite is represented as the major calcium carbonate phase and remains stable even after exposure to the model solution for 120 h. Hence, we may suggest that the specific effect on phase formation and the stability of calcium carbonate is caused by some of the EAAs or a combination of several amino acids with one another, with albumen, or with bile components.

Even though modern knowledge of the pathophysiology of cholelithiasis has recently expanded, the methods of treatment remain invasive and based on surgical intervention [44-47]. Thus, in the future, the efforts of scientists should be directed at finding new preventive strategies to prevent the occurrence of stone formation among the entire population of the world.

Conclusion

As a result of the thermodynamic modeling of the formation of calcium carbonate in a model solution of bile (inorganic composition), it was found that during the functioning of the human body, crystallization of calcium carbonate normally does not occur. The occurrence of local high supersaturations of precipitate-forming ions in bile can lead to the formation of $CaCO_3$ solid-phase nuclei and further crystallization of gallstones.

Calcium carbonate was synthesized from bile-containing solutions. It was determined that the samples synthesized in the absence of bile and with a concentration of 1 mass % contained calcite. An increase in bile content in the initial solution from 5 to 100 mass % promotes vaterite crystallization. Studies of the effect of bile on the mass of the solid phase showed that the mass of the precipitate increases in proportion to an increase in bile concentration in the initial solution. Investigation of the dissolution of synthesized samples in NaCl (0.9 mass %) and EDTA (0.05 mol/L) solutions revealed that the presence of bile components in the solid samples causes a decrease in the rate of their dissolution.

Performing experimental modeling of calcium carbonate crystallization in a human bile model solution, we found that essential amino acids virtually do not affect the formation of low-soluble compounds ($CaCO_3$), but they yet change the qualitative phase composition of the resulting powders. When present in average physiological concentrations, glycine, glutamic acid, and albumen separately do not modify the composition of the synthesized samples relative to the calcium carbonate obtained in a pure bile model solution. However, when their concentrations increase to the highest values permissible for their joint presence, they enhance the formation of vaterite, the metastable calcium carbonate polymorph, as the major phase.

Acknowledgement

The was work by under project within the framework of an additional agreement to the agreement on the provision of subsidies from the federal budget for financial support for the implementation of the state task No. 075-03-2023.

References

1. Di Ciaula A, Wang DQ, Portincasa P. An update on the pathogenesis of cholesterol gallstone disease. Curr Opin Gastroenterol. 2018 Mar;34(2):71-80. doi: 10.1097/MOG.0000000000000423. PMID: 29283909; PMCID: PMC8118137

2. Portincasa P, Di Ciaula A, de Bari O, Garruti G, Palmieri VO, Wang DQ. Management of gallstones and its related complications. Expert Rev Gastroenterol Hepatol. 2016;10(1):93-112. doi: 10.1586/17474124.2016.1109445. Epub 2015 Nov 11. PMID: 26560258.

3. Shabanzadeh DM, Sørensen LT, Jørgensen T. Determinants for gallstone formation - a new data cohort study and a systematic review with meta-analysis. Scand J Gastroenterol. 2016 Oct;51(10):1239-48. doi: 10.1080/00365521.2016.1182583. Epub 2016 May 27. PMID: 27232657.

4. Di Ciaula A, Portincasa P. Diet and Contaminants: Driving the Rise to Obesity Epidemics? Curr Med Chem. 2019;26(19):3471-3482. doi: 10.2174/0929867324666170518095736. PMID: 28521687.

5. Golovanova OA. Gallstones: monograph. Omsk: Publishing House "Science"; 2012. 126 p.

6. Svistunov AA, Osadchuk MA, Kireeva NV, Osadchuk AM. Gallstone disease as a clinical marker of metabolic syndrome. Obesity and metabolism. 2018;15(3):3-8. https://doi.org/10.14341/omet9553.

7. Liu Z, Kemp TJ, Gao YT, Corbel A, McGee EE, Wang B, Shen MC, Rashid A, Hsing AW, Hildesheim A, Pfeiffer RM, Pinto LA, Koshiol J. Association of circulating inflammation proteins and gallstone disease. J Gastroenterol Hepatol. 2018 Nov;33(11):1920-1924. doi: 10.1111/jgh.14265. Epub 2018 May 17. PMID: 29671891; PMCID: PMC7576672.

8. Gupta A, Gupta S, Siddeek RAT, Chennatt JJ, Singla T, Rajput D, Kumar N, Sehrawat A, Kishore S, Gupta M. Demographic and clinicopathological Profile of Gall Bladder Cancer Patients: Study from a tertiary care center of the Sub-Himalayan region in Indo-Gangetic Belt. J Carcinog. 2021 Jun 9;20:6. doi: 10.4103/jcar.JCar_3_21. PMID: 34321956; PMCID: PMC8312375.

9. Schmidt MA, Marcano-Bonilla L, Roberts LR. Gallbladder cancer: epidemiology and genetic risk associations. Chin Clin Oncol. 2019 Aug;8(4):31. doi: 10.21037/cco.2019.08.13. PMID: 31484487.

10. Metvalli KA. Physical and chemical laws of synthesis of submicron particles of vaterite and their application in composites. Abstract Dissertation. 2015;25.

11. Ivashkin VT. Gastroenterology. Moscow: GEOTAR-Media; 2015;250.

12. Dutta A, Mungle T, Chowdhury N, Banerjee P, Gehani A, Sen S, Mallath M, Roy P, Krishnan S, Ganguly S, Banerjee S, Roy M, Saha V. Characteristics and outcomes of gallbladder cancer patients at the Tata Medical Center, Kolkata 2017-2019. Cancer Med. 2023 Apr;12(8):9293-9302. doi: 10.1002/cam4.5677. Epub 2023 Feb 13. PMID: 36779618; PMCID: PMC10166897.

13. Shenoy R, Mederos MA, Ye L, Mak SS, Begashaw MM, Booth MS, Shekelle PG, Wilson M, Gunnar W, Maggard-Gibbons M, Girgis MD. Intraoperative and postoperative outcomes of robot-assisted cholecystectomy: a systematic review. Syst Rev. 2021 Apr 23;10(1):124. doi: 10.1186/s13643-021-01673-x. PMID: 33892794; PMCID: PMC8067374.

14. He M, Shi B. Gut microbiota as a potential target of metabolic syndrome: the role of probiotics and prebiotics. Cell Biosci. 2017 Oct 25;7:54. doi: 10.1186/s13578-017-0183-1. PMID: 29090088; PMCID: PMC5655955.

15. Holcomb M, Cohen AL, Gabitov RI, Hutter JL. Compositional and morphological features of aragonite precipitated experimentally from seawater and biogenically by corals. Geochim Cosmochim Acta. 2009;4166-4179.

16. Kawano J, Sakuma H, Nagai T. Incorporation of Mg2+ in surface Ca2+ sites of aragonite: an ab initio study. Prog Earth Planet Sci. 2015;2.

17. Mass T, Giuffre AJ, Sun CY, Stifler CA, Frazier MJ, Neder M, Tamura N, Stan CV, Marcus MA, Gilbert PUPA. Amorphous calcium carbonate particles form coral skeletons. Proc Natl Acad Sci U S A. 2017 Sep 12;114(37):E7670-E7678. doi: 10.1073/pnas.1707890114. Epub 2017 Aug 28. PMID: 28847944; PMCID: PMC5604026.

18. Purgstaller B, Dietzel M, Baldermann A, Mavromatis V. Control of temperature and aqueous Mg2+/Ca2+ ratio on the (trans-) formation of ikaite. Geochim Cosmochim Acta. 2017;217:128-143.

19. Purgstaller B, Mavromatis V, Immenhauser A, Dietzel M. Transformation of Mg-bearing amorphous calcium carbonate to Mg-calcite – In situ monitoring. Geochim Cosmochim Acta. 2016;174:180-195.

20. Mavromatis V, Immenhauser A, Buhl D, Purgstaller B, Baldermann A, Dietzel M. Effect of organic ligands on Mg partitioning and Mg isotope fractionation during low-temperature precipitation of calcite in the absence of growth rate effects. Geochim Cosmochim Acta. 2017;207:139-153.

21. Uchikawa J, Harper DT, Penman DE, Zachos JC, Zeebe RE. Influence of solution chemistry on the boron content in inorganic calcite grown in artificial seawater. Geochim Cosmochim Acta. 2017;218:291-307.

22. Declet A, Reyes E, Suarez OM. Calcium carbonate precipitation: a review of the carbonate crystallization process and applications in bioinspired. Nanotechnology Center for Biomedical, Environmental and Sustainability Applications. 2015;21.

23. Golovanova OA. Crystallogenesis in the human body. Omsk: Publishing house Dostoevsky Omsk State University; 2022. 350 p.

24. Golovanova OA, Korol'kov VV. Thermodynamics and kinetics of calcium oxalate crystallization in the presence of amino acids. Crystallography Reports. 2017;62(5):787-796.

25. Golovanova OA. Thermodynamic modeling of poorly soluble compounds formation in biological fluid. J Thermal Anal Calorim. 2018;133(2):1219.

26. Mashina EV, Makeev BA, Filippov VN. Calcium carbonates in choleliths. J Proceedings of the Tomsk Polytechnic University. 2015;326(1):34-39.

27. speciation in calcite and aragonite from co-precipitation experiments under controlled pH, temperature and precipitation rate. Geochim Cosmochim Acta. 2015;150:299-313.

28. Azatyan KA, Alekseev AV, Zubareva GM. Study of the composition of gallstones and methods of their dissolution. Successes of modern natural science. 2013;12-17.

29. Uchikawa J, Penman DE, Zachos JC, Zeebe RE. Experimental evidence for kinetic effects on B/Ca in synthetic calcite: Implications for potential B(OH)4- and B(OH)3 incorporation. Geochim Cosmochim Acta. 2015;150:171-191.

30. Voigt M, Mavromatis V, Oelkers EH. The experimental determination of REE partition coefficients in the water-calcite system. Chem Geol. 2017;462:30-43.

31. Haynes WM, ed. CRC Handbook of Chemistry and Physics. 97th ed. Boca Raton: CRC Press; 2010. 2760 p.

32. Golovanova OA, Leonchuk SS. Synthesis of Calcium Carbonate in the Presence of Bile, Albumen, and Amino Acids. Russ J Inorg Chem. 2020;65(4):472-479. https://doi.org/10.1134/S0036023620040063.

33. Golovanova OA, Korol'kov VV. Thermodynamics and kinetics of calcium oxalate crystallization in the presence of amino acids. Crystallography Reports. 2017;62(5):787-796.

34. Golovanova OA, Korol'kov VV, Punin YO, Izatulina AR. Crystallization of calcium oxalate monohydrate in the presence of amino acids: Features and regularities. J Struct Chem. 2014;55(7):1356-1370.

35. Rollion-Bard C, Blamart D. Possible controls on Li, Na, and Mg incorporation into aragonite coral skeletons. Chem Geol. 2015;396:98-111.

36. Poulain C, Gillikin DP, Thebault J, Munaron JM, Bohn M, Robert R, Paulet YM, Lorrain A. An evaluation of Mg/Ca, Sr/Ca, and Ba/Ca ratios as environmental proxies in aragonite bivalve shells. Chem Geol. 2015;396:42-50.

37. Poudel L, Tamerler C, Misra A. Atomic-Scale Quantification of Interfacial Binding between Peptides and Inorganic Crystals: The Case of Calcium Carbonate Binding Peptide on Aragonite. J Phys Chem C. 2017;121(51):28354. https://doi.org/10.1021/acs.jpcc.7b10004.

38. Wehrmeister U. Raman spectroscopy of synthetic, geological and biological vaterite: a Raman spectroscopic study. J Raman Spectrosc. 2010;41:193–201.

39. Golovanova OA, Tsyganova AA, Chikanova ES. Directed synthesis of octacalcium phosphate and investigation of its properties. Glass Phys Chem. 2016;42(6):798-806.

40. Matton APM, de Vries Y, Burlage LC, van Rijn R, Fujiyoshi M, de Meijer VE, de Boer MT, de Kleine RHJ, Verkade HJ, Gouw ASH, Lisman T, Porte RJ. Biliary Bicarbonate, pH, and Glucose Are Suitable Biomarkers of Biliary Viability During Ex Situ Normothermic Machine Perfusion of Human Donor Livers. Transplantation. 2019 Jul;103(7):1405-1413. doi: 10.1097/TP.0000000000002500. PMID: 30395120; PMCID: PMC6613725.

41. Tomashevskiy IA, Golovanova OA, Anisina SV. Coordination Compounds of Calcium Ions (II) with the Biogenic Amino Acids: Their Stability, Kinetic and Thermodynamic Characteristics of the Formation. In: Processes and phenomena on the boundary between biogenic and abiogenic nature. 2020;765-782. DOI: 10.1007/978-3-030-21614-6_41.

42. Golovanova OA. Crystallization of Calcium Carbonates from Solutions Containing Bile. Chem Sustain Dev. 2021;29(1):26-33. DOI: 10.15372/CSD2021274.

43. Janowitz P, Mason R, Kratzer W. Stability of human gallbladder bile: effect of freezing. Can J Gastroenterol. 2001 Jun;15(6):363-6. doi: 10.1155/2001/952683. PMID: 11429664.

44. Franke VD, Bocharov SN. Morphology of calcium carbonate crystals in

the presence of aspartic acid, gelatin, and cholesterol. In: Proceedings of the 11th Congress of the Russian Medicinal Society, St. Petersburg, 2010; 160.

45. Lammert F, Gurusamy K, Ko CW, Miquel JF, Méndez-Sánchez N, Portincasa P, van Erpecum KJ, van Laarhoven CJ, Wang DQ. Gallstones. Nat Rev Dis Primers. 2016 Apr 28;2:16024. doi: 10.1038/nrdp.2016.24. PMID: 27121416.

46. Sharma S, Walia BS, Randhawa M, Sharma A, Dugg P, Pannu JS. Histopathological changes in gall bladder mucosa in relation to the number, and size of gallstones, and analysis of the findings in the context of age distribution of the patients: A perspective. Ann Hepatobiliary Pancreat Surg. 2023 Aug 31;27(3):277-286. doi: 10.14701/ahbps.23-010. Epub 2023 Aug 7. PMID: 37547937; PMCID: PMC10472125.

47. Hyun JJ, Lee HS, Kim CD, Dong SH, Lee SO, Ryu JK, Lee DH, Jeong S, Kim TN, Lee J, Koh DH, Park ET, Lee IS, Yoo BM, Kim JH. Efficacy of Magnesium Trihydrate of Ursodeoxycholic Acid and Chenodeoxycholic Acid for Gallstone Dissolution: A Prospective Multicenter Trial. Gut Liver. 2015 Jul;9(4):547-55. doi: 10.5009/gnl15015. PMID: 26087862; PMCID: PMC4478000.

How to cite this article: Golovanova O. Biomimetic Synthesis of Calcium Carbonate in Bile in the presence of Amino Acids. IgMin Res. July 18, 2024; 2(7): 632-641. IgMin ID: igmin227; DOI: 10.61927/igmin227; Available at: igmin.link/p227